

Crystalline Nanoscale Assembly of Gold Clusters for Reversible Storage and Sensing of CO₂ via Modulation of Photoluminescence Intermittency

Srestha Basu,^a Satyapriya Bhandari,^b Uday Naryan Pan,^a Anumita Paul*^a and Arun

Chattopadhyay*^{a,b}

^aDepartment of Chemistry, ^b Centre for Nanotechnology

Indian Institute of Technology Guwahati, Guwahati-781039, Assam, India.

*E-mail: arun@iitg.ernet.in, anumita@iitg.ernet.in

Electronic Supplementary Information

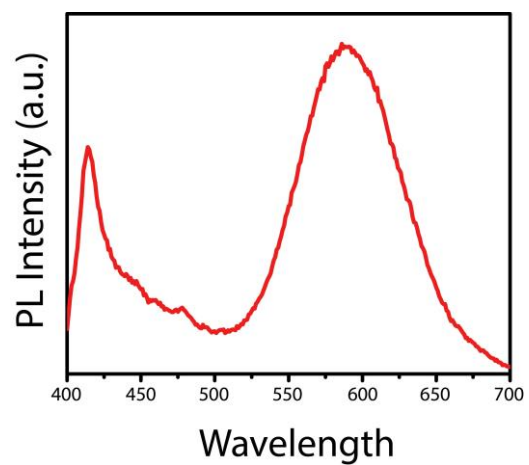


Fig. S1 Emission spectrum (λ_{ex} - 355 nm) of the as-synthesized Cys-Au₁₄ NCs.

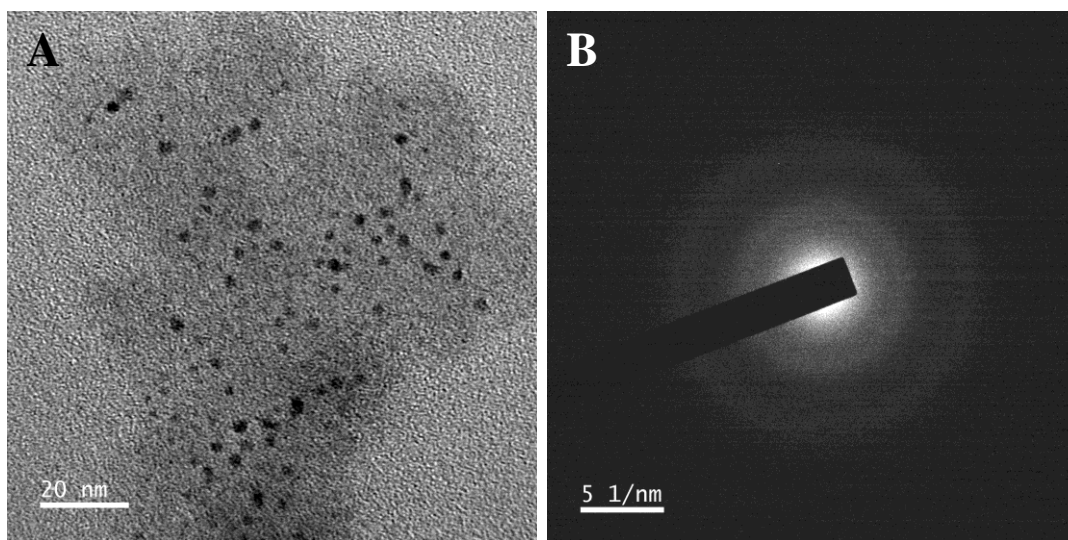


Fig. S2 (A) Transmission electron microscopy (TEM) image and (B) selected area electron diffraction (SAED) pattern of the as-synthesized Cys-Au₁₄ NCs.

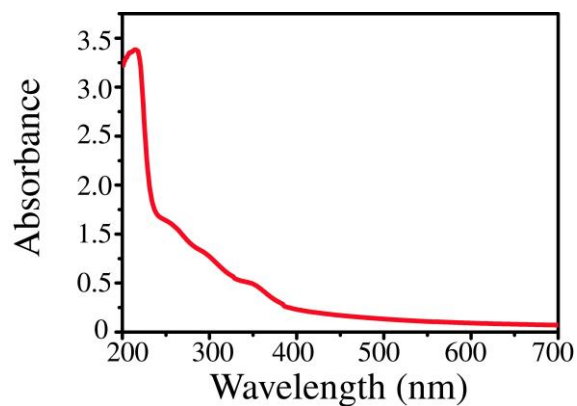


Fig. S3 Absorption spectrum of the Cys-Au₁₄ NCs.

Sample Name	Unavailable	Position	Unavailable	Instrument Name	Unavailable	User Name	Unavailable
Inj Vol	Unavailable	InjPosition	Unavailable	SampleType	Unavailable	IRM Calibration Status	All Ions Missed
Data Filename	CYS AU NCS.d	ACQ Method		Comment	Sample information is unavailable	Acquired Time	Unavailable

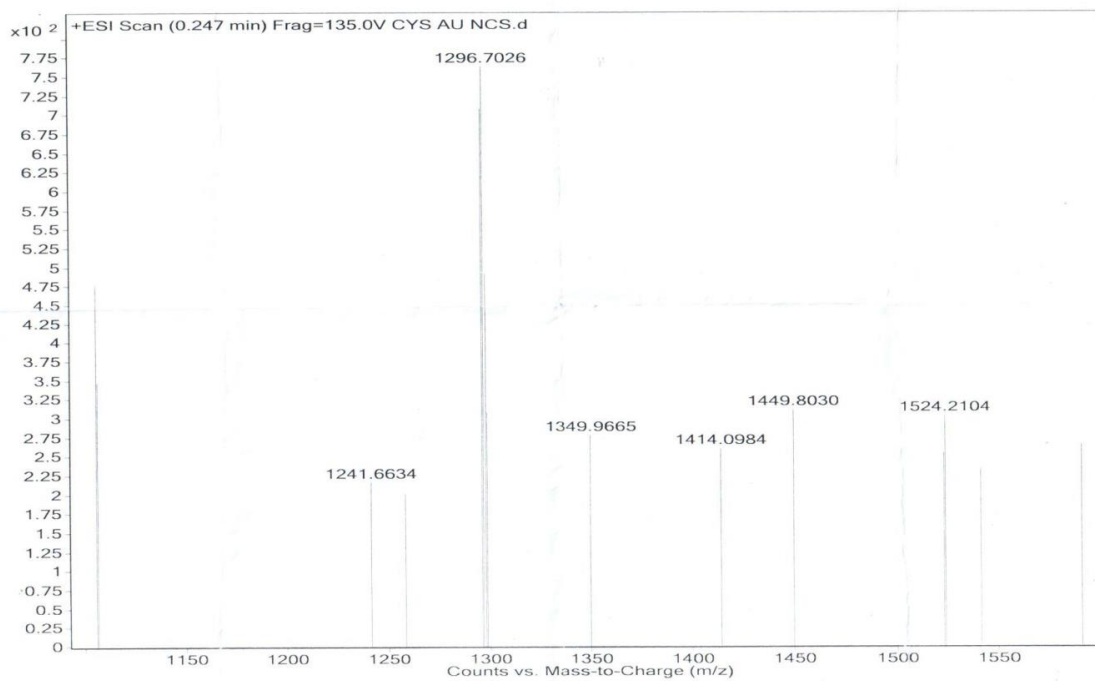


Fig. S4 Electrospray Ionization mass spectrum (ESI-MS) of Cys-Au₁₄ NCs.

Table S1. Mass fragments corresponding to the observed peaks in ESI-MS of the as-synthesized Cys-Au₁₄ NCs. This clearly indicated the successful formation of Au₁₄ NCs with the molecular formula Au₁₄MPA₁₀Cys₄.

Peak position	Component
1449.80	[Au ₁₄ MPA ₁₀ Cys ₄ + 3 Na ⁺] ³⁺
1241.66	[Au ₁₄ MPA ₄ Cys ₄ + 3 Na ⁺] ³⁺
1414.09	[Au ₁₄ MPA ₉ Cys ₄ + 3 Na ⁺] ³⁺
1296.70	[Au ₁₄ MPA ₉ Cys + 3 Na ⁺] ³⁺
1349.96	[Au ₁₄ MPA ₁₀ Cys ₂ + 3 H ⁺] ³⁺
1524.21	[Au ₁₄ Cys ₂ + 2 Na ⁺] ²⁺

Explaining the stability of Au₁₄MPA₁₀Cys₄ on the basis of superatom model

Electro spray ionization mass spectrometric analysis revealed the molecular formula of cysteine protected Au₁₄ clusters to have been Au₁₄MPA₁₀Cys₄ with MPA denoting mercaptopropionic acid and cys representing cysteine.

The number of superatomic electrons in the clusters is given by the following formula:

$$N^* = NV_A - M - Z;$$

(Where N = number of atoms in the cluster; V = 1 for gold; M = Number of electron withdrawing ligands; Z = overall charge on the compound)

Considering the molecular formula of the clusters to be Au₁₄MPA₁₀Cys₄,

$$N = 14,$$

$$M = \text{number of cysteine} = 4$$

(It has been stated in the earlier version of the manuscript that MPA – Au defines emissive states while Cys- Au defines dark states. This is attributed to electron withdrawing ability of cysteine molecules.)

Z= 10 due to 10 deprotonated carboxylate groups of MPA molecules. It is worth mentioning here that cysteine under the pH of the medium remains charge neutral. Hence overall charge on the molecule is -10.

Thus, $N^* = 14 - 4 - (-10) = 20$; which corresponds to stable electron configuration as per “Aufbau rule of metal nanoclusters” with the configuration being $1S^2 1P^6 1D^{10} 2S^2$.¹

Thus the calculation shows that the Au_{14} nanoclusters with the stabilizing ligands used herein could be considered as a stable species for the formation of higher order structure.

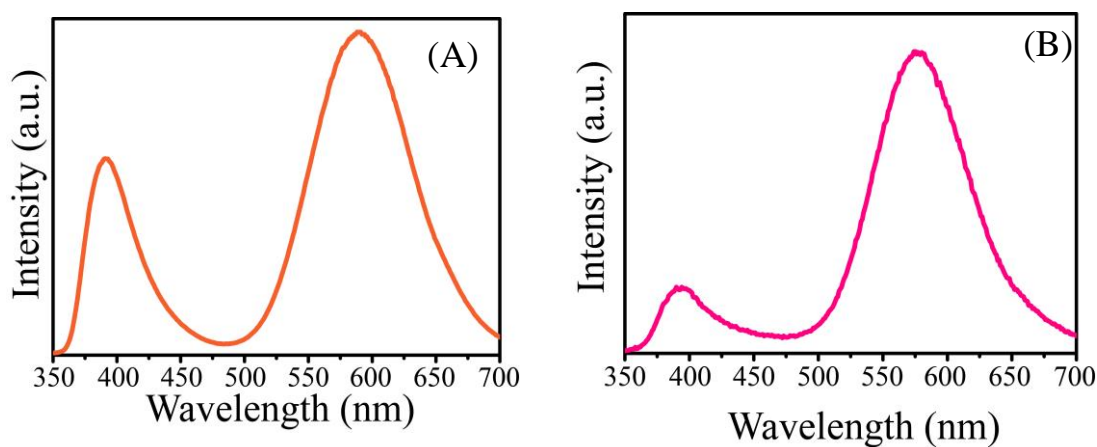


Fig. S5 Emission spectra (λ_{ex} - 355 nm) of the as-synthesized (A) Trp- Au_{14} NCs and (B) His- Au_{14} NCs.

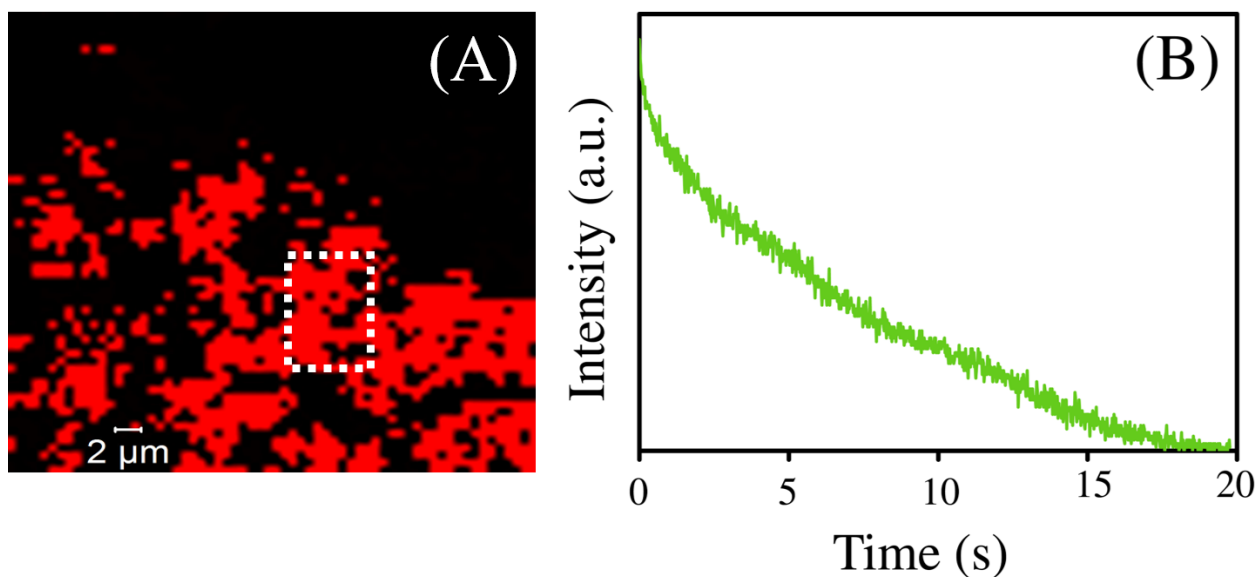


Fig. S6 (A) Confocal laser scanning microscopic image and (B) time dependent photoluminescence intermittency profile (which was recorded against marked portion in Fig. S6A) of aggregated Cys-Au₁₄ NCs. The blinking profile was recorded using a fixed binning time of 27 ms and with excitation power of 63 mW (wavelength of 355 nm) for a time span of 20 s.

Table S2. Fitting parameters (as per the data obtained from Fig. 1) for probability density of *off*-states ($\rho_{\text{off}}(t)$) for (A) Cys-Au₁₄ (B), Trp-Au₁₄ and (C) His-Au₁₄ NCs.

Equation: $\rho_i(\tau) = A\tau^{-\alpha} \exp(-\mu\tau)$

Sample	α_{off}	μ_{off}	A_{off}	χ^2
(A) Cys – Au ₁₄ NCs	0.32 ± 0.06	6.9 ± 0.86	124.7 ± 32.2	0.99
(B) His - Au ₁₄ NCs	0.17 ± 0.06	7.2 ± 0.8	67.9 ± 17.06	0.99
(C) Trp - Au ₁₄ NCs	0.49 ± 0.03	5.8 ± 0.47	88.4 ± 12.58	0.99

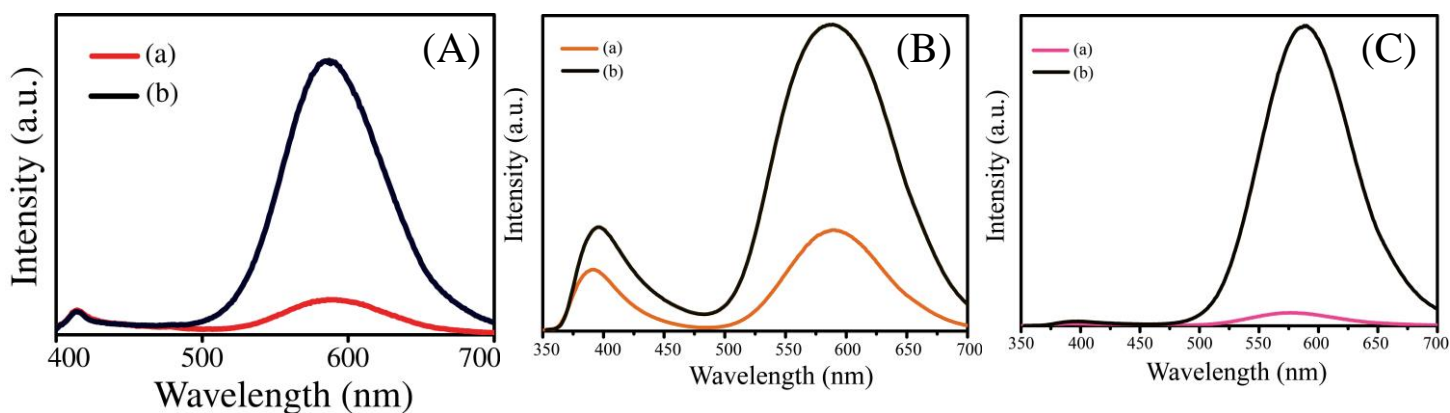


Fig. S7. Emission spectra (λ_{ex} - 355 nm) of as-synthesized (A) Cys-Au₁₄ NCs, (B) Trp-Au₁₄ NCs and (C) His-Au₁₄ NCs (a) before and (b) after complexation with Zn²⁺ ions.

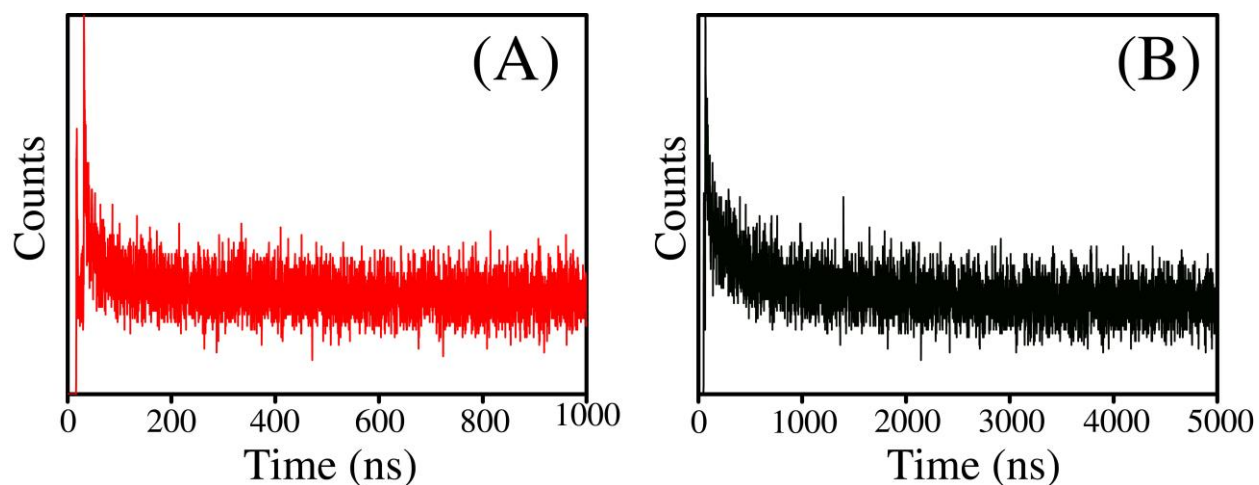


Fig. S8. Time-resolved photoluminescence spectra (recorded using 375 nm excitation laser) of as-synthesized (A) Cys-Au₁₄ NCs and (B) Cys-Au₁₄ NCs following complexation with Zn²⁺ ions.

Table S3. Average emission life times calculated from the time resolved photoluminescence spectra (recorded using 375 nm excitation laser) of as-synthesized (A) Cys-Au₁₄ NCs and (B) Cys-Au₁₄ NCs following complexation with Zn²⁺ ions.

Sample	A ₁ (%)	τ ₁ (ns)	A ₂ (%)	τ ₂ (ns)	χ ²
(A) Cys-Au ₁₄ NCs	41.1	7.01	58.9	142.5	1.03
(B) Zn-Cys-Au ₁₄ NCs	22.2	44.1	77.8	846.1	1.07

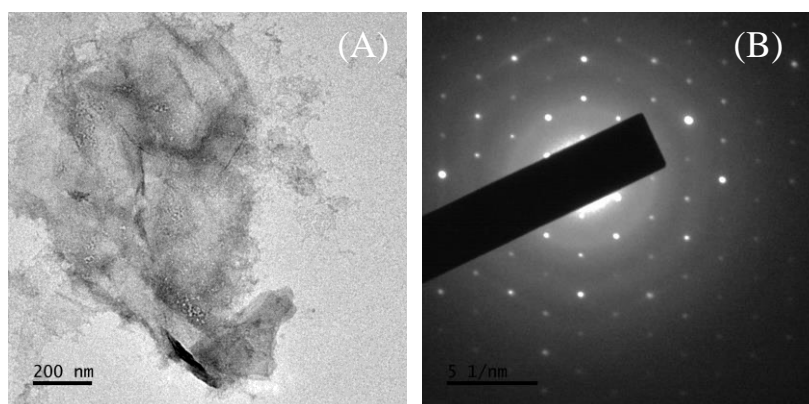


Fig. S9 (A) Transmission electron microscopy (TEM) image and (B) corresponding selected area electron diffraction (SAED) pattern of Zn-Cys-Au₁₄-NCs. These images are for additional crystal similar to the one in Fig. 2, which reflected the reproducibility of the results.

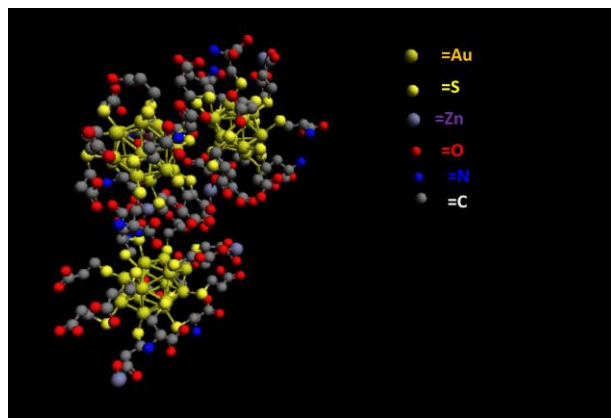


Fig. S10 Computationally optimized structure of Zn-Cys-Au₁₄-NC complex obtained using Avogadro software. Hydrogen atoms have not been included for simplicity.

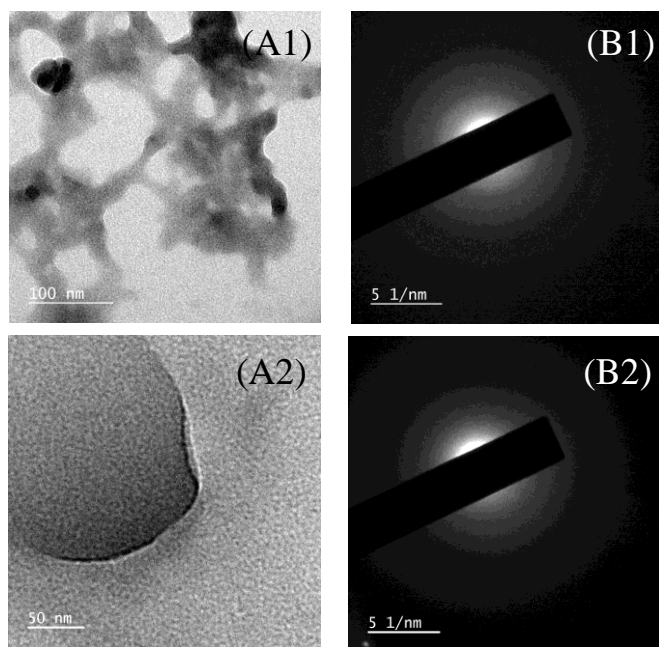


Fig. S11 (A) Transmission electron microscopy (TEM) images and **(B)** selected area electron diffraction (SAED) patterns of the evaporated dispersion containing Cys, MPA and Zn²⁺ ions and acquired at two different positions (1 and 2) of the sample.

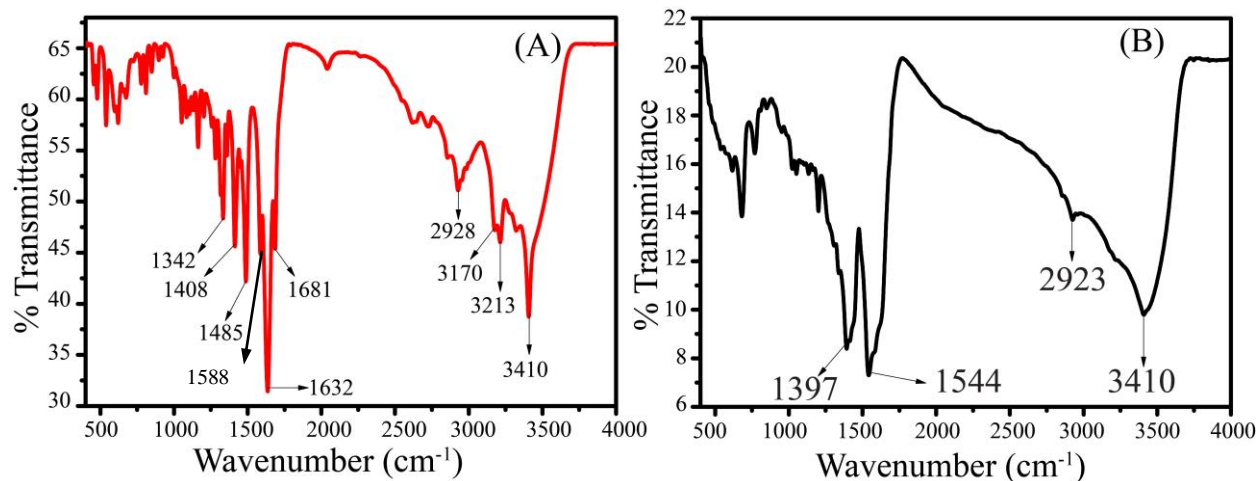


Fig. S12. FTIR spectra of (A) Cys-Au₁₄ NCs and (B) Zn-Cys-Au₁₄ NCs.

FTIR analysis: It is interesting to note that the peak due to asymmetric stretch of carboxylate group of MPA attached to Cys-Au₁₄ NCs at 1681 cm⁻¹ was absent in the FTIR spectrum of Zn-Cys-Au₁₄-NCs. This indicates possible binding of MPA with zinc ions through the carboxylate group of the former. Additionally, the peak due to asymmetric stretch of cysteine at 1588 cm⁻¹ was shifted to 1544 cm⁻¹ upon complexation with zinc ions thereby indicating possible binding of cysteine attached to Cys-Au₁₄ NCs with zinc ions via the carboxylate group of the former. Also, the peaks due to symmetric stretches of carboxylate group of MPA and cysteine attached to Cys-Au₁₄ NCs were observed to have been dampened upon complexation with zinc ions. The non-involvement of the amine group of cysteine in complexation with zinc ions was confirmed from the observation that the peak position due NH₃⁺ at 3410 cm⁻¹ practically remained unaltered upon complexation with zinc ions.

Structural details of Zn-Cys-Au₁₄-NCs - Concisely, a regular hexagon is formed comprising of six flat 3D Au₁₄ NCs (with D_{2h} symmetry)² at the apexes and one Au₁₄ NC at the center. The two NCs at the apexes and the one at the center are connected via Zn²⁺ ion coordinated to MPA ligated to the Au atoms constituting the NCs. Hence, a two dimensional hexagonal layer is formed where each hexagon comprises of seven Au₁₄ NCs and three Zn²⁺ ions. The distance between each Au₁₄ NCs forming the hexagon (i.e., the edge length of the hexagon) has been computed to be 4.4 Å, which is close to the observed value of 4.7 ± 0.2 Å. On the other hand, vertically, the NCs are linked through Cys molecules attached to the Au₁₄ NCs via coordination through Zn²⁺ ions. The cluster to cluster distance in the vertical dimension has been calculated to be 8.7 Å, which is in close concordance with the observed value of 8.4 Å. Moreover, in the vertical direction, the distance between Au₁₄-Cys-Zn-Cys-Au₁₄-Cys-Zn has been calculated to be 17.2 Å. Further, Zn-Cys distance has been observed to be 6.3 Å which when added to 17.2 Å is close to the observed value of 22 Å and hence defines the repeat unit in the crystal.

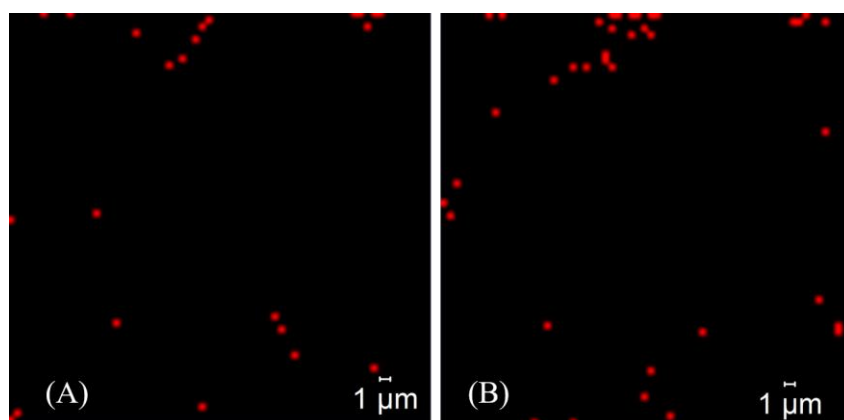


Fig. S13 Confocal laser scanning microscopic image of (A) Cys-Au₁₄ NCs and the same sample following (B) purging by 2.5% CO₂.

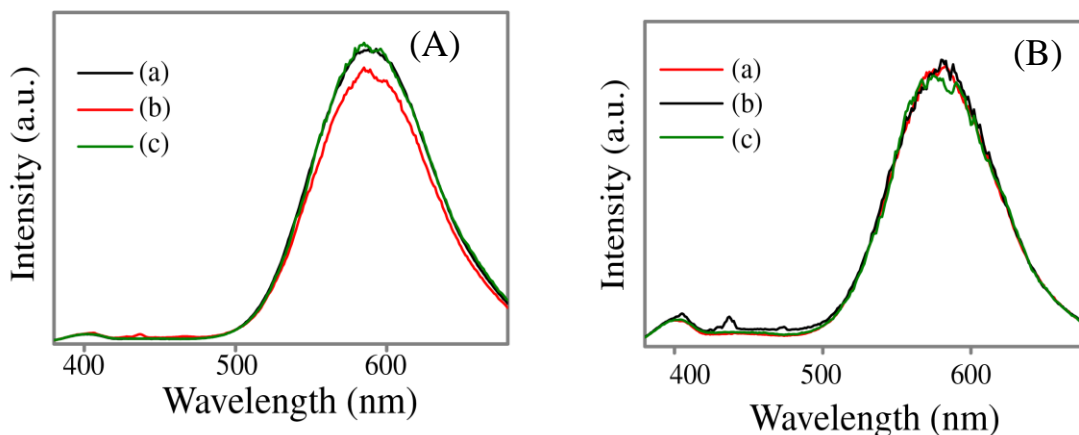


Fig. S14 (A) Photoluminescence spectrum of (a) aqueous dispersion of Zn-Cys-Au₁₄ NCs and that same sample following (b) purging by CO₂ and then (c) release of CO₂. **(B)** Photoluminescence spectrum of (a) Cys-Au₁₄ NCs, and the same sample following (b) purging by CO₂ and then (c) release of CO₂. The excitation wavelength was fixed at 355 nm.

Additional Figures and discussions:

Origin of luminescence in Cys-Au NCs. The origin of the emission at 590 nm is likely to have occurred from a metal ligand emission state. As per studies of Goodson and co-workers⁵ relaxation pathway in a typical cluster primarily involves five states:

- (i) A ground state
- (ii) A core state (akin to excited state in case of molecular fluorophores)
- (iii) An intermediate state associated with the core state
- (iv) A dark state
- (v) A metal-ligand emission state

In a typical relaxation process, following excitation from the ground state to the core state, the system initially relaxes to an intermediate state. This relaxation is often referred to

as “fast relaxation” and occurs on an ultrafast time scale. At this stage, three possibilities exist:

- (i) A fast emission to the ground state referred to as “fast core emission”.
- (ii) Transition to a dark state. Relaxation from the above mentioned intermediate state to the dark state has been proposed to occur via intracluster non-radiative transitions.
- (iii) Transition to an emissive metal ligand state.

However, this emission is proposed to have originated from the ligands stabilizing the clusters and has no direct contribution from the clusters. It may be noted that the ligands stabilizing the clusters are amino acids (cysteine, histidine and tryptophan) in all three cases. Thus, their intrinsic emission is likely to be preserved even after coordination to the Au atoms of the clusters. In order to establish this statement, we have performed control experiments of cysteine, tryptophan and histidine. Interestingly, in all three cases, the emission at ~410 nm with a sharp feature at 400 nm could be observed (Fig. S15). It is to be noted here that the variation in intensity is attributed to the different concentration of the amino acids used during measurement.

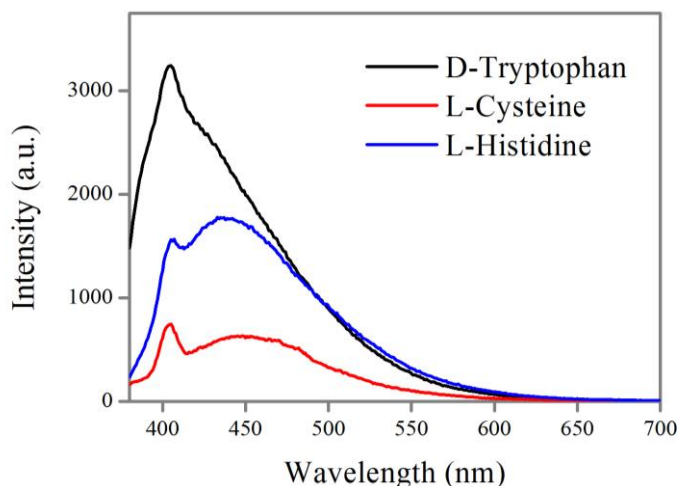


Fig. S15: Emission spectra of L-cysteine, L histidine and D tryptophan. λ_{exc} was set at 355 nm.

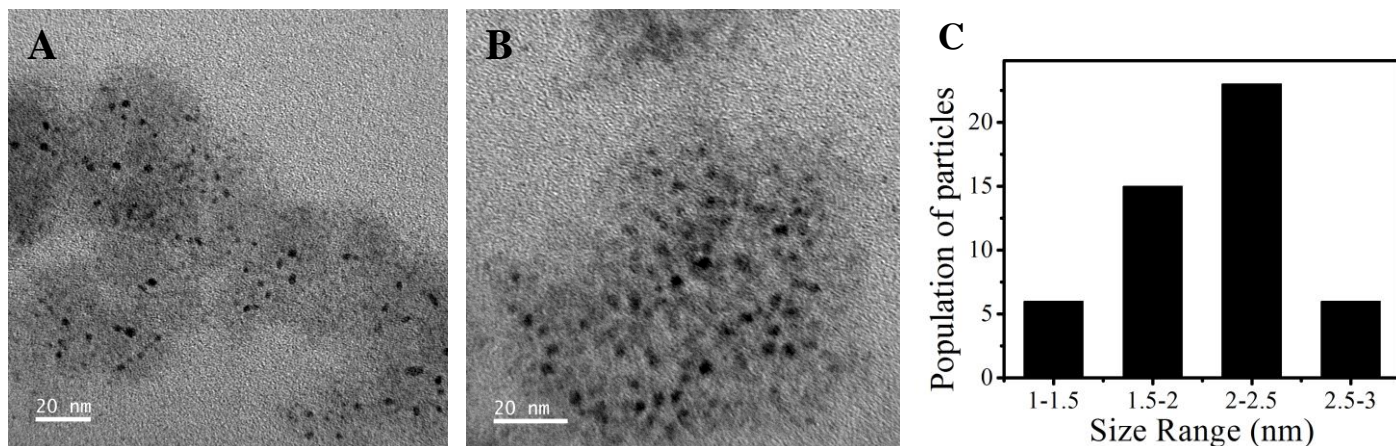


Fig. S16. (A-B) Additional TEM images of Cys Au NCs and (C) corresponding size distribution.

Control experiments and explanations to eliminate the interference of detector noise in the intermittency signals of Cys Au NCs

In the CLSM model used for pursuing the current study (Zeiss LSM 880), range indicator is used to specify the area of luminescence and that of background in a particular frame of measurement. By default, red portions indicate non-zero or high pixel values and blue portions are indicative of zero pixel values.³

Also, in the confocal setup (LSM 880), gain master is adjusted to maximize the signal to noise ratio in a particular measurement. Herein, an optimized gain master of value 833 has been used to eliminate the background noise and acquire noise free images. Thus we have recorded a CLSM image of the background (recorded without inserting any sample), at a gain master of 833, with the range indicator being enabled. In an allied vein, we have recorded the CLSM image of Cys Au NCs along with background with the range indicator enabled. Interestingly, while in case of the background (only) the entire frame appeared blue indicating no detectable signal (Fig. S17 A-B), in case of Cys Au NCs, the area comprising of the clusters

appeared red and the background (where absence of clusters was anticipated) appeared blue (Fig. S17 C-D).

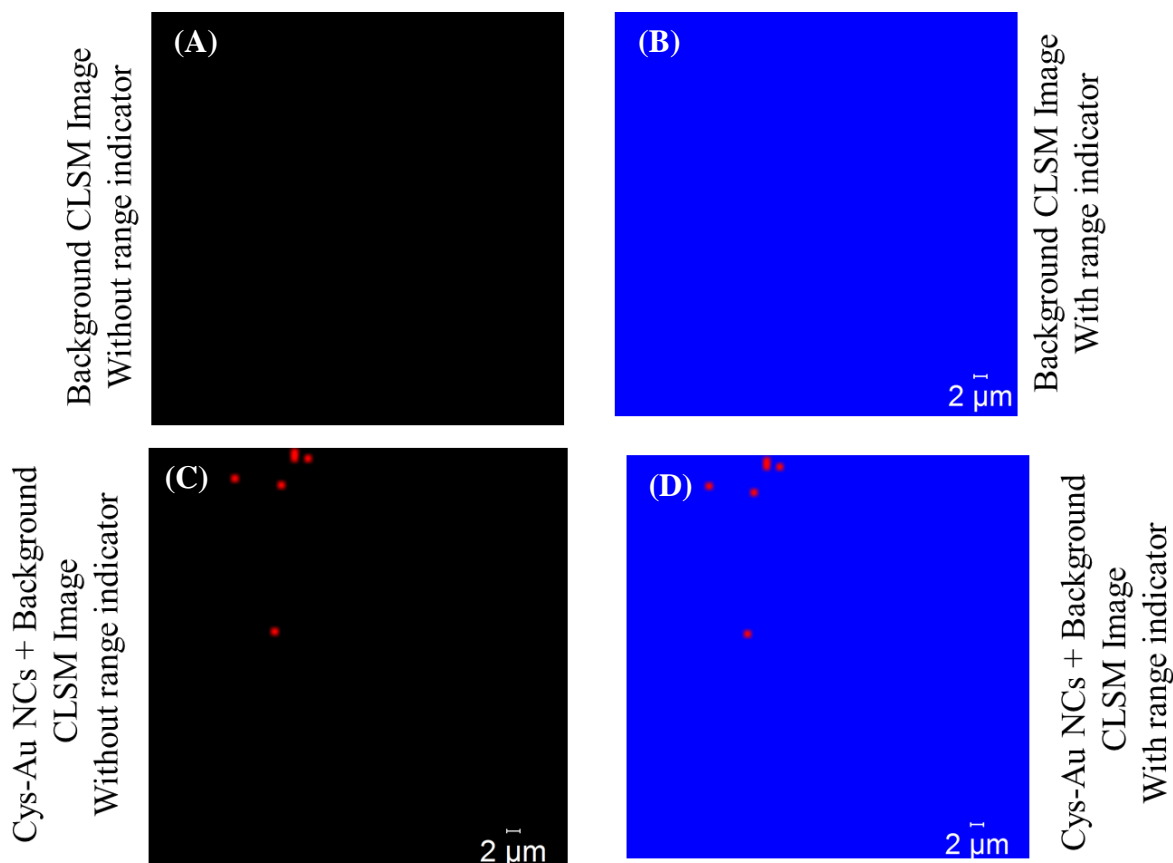


Fig. S17. (A) Confocal laser scanning microscopic image of a background (recorded without inserting any sample). (B) Corresponding image of background with range indicator being enabled. (C) Confocal laser scanning microscopic image of Cys Au NCs in presence of background (D) Corresponding image Cys Au NCs in presence of background with range indicator being enabled.

Secondly, in order to establish that the reported images and the blinking profiles are typical signatures of the luminescent clusters, we have acquired the luminescent spectrum on a typical particle of Cys Au NCs. Similarly, we have acquired the spectrum of the background in the same frame as that of the clusters. It is worthy to be mentioned here that the acquisitions have

been done at a gain master value of 833. This value was optimized to completely eliminate the interference of background. Details of the optimization process is discussed in the subsequent section. Interestingly, in case of clusters, the spectrum matched exactly with that of the solution phase, exhibiting an emission maximum at 589 nm. On the other hand, the spectrum acquired on the background was devoid of any characteristic peak at ~ 590 nm (Fig. S18).

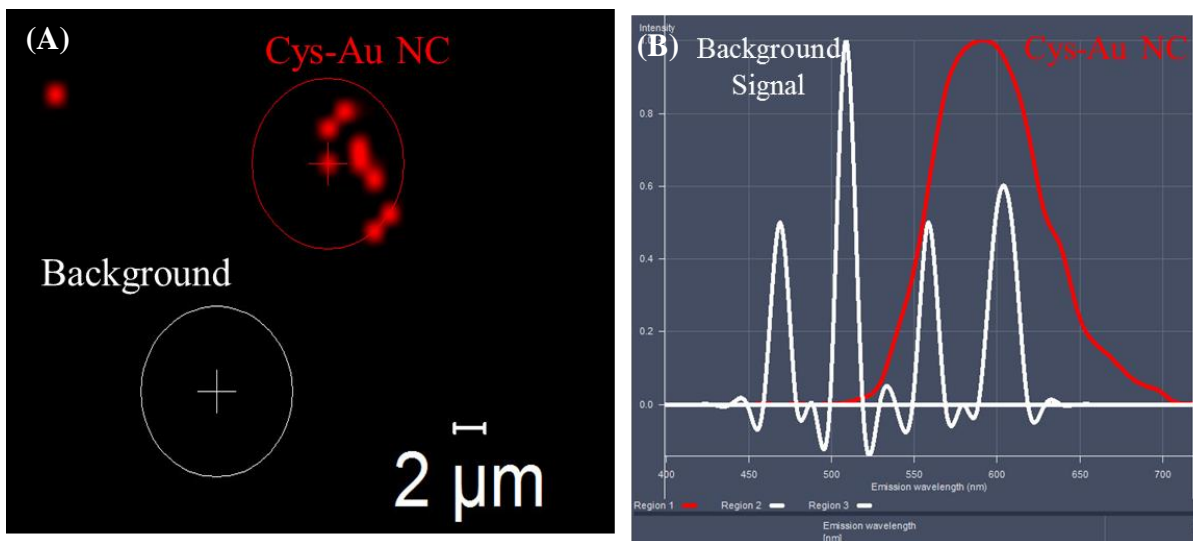


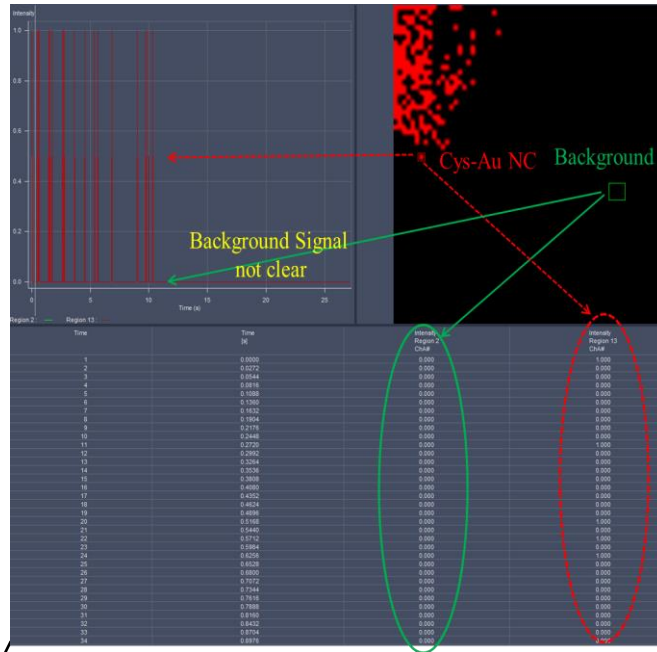
Fig. S18. (A) CLSM image of Cys Au NCs (B) Corresponding spectra acquired on the regions marked in (A). The instrument displays the emission spectrum in the scale of 1.0 for all measurements.

Thirdly, it was observed that the interference of the detector noise could be tuned by adjusting the value of gain master. Intriguingly, acquiring the blinking of profile of the background (without using any sample) at a gain master of 833, no signal from background could be observed. However, upon increasing the gain master to 1000, background signals could be observed (The results are shown in Fig. S21-S22 in subsequent section). Nevertheless, the value of the intensity of the background profile was 10^{-3} times of that of the clusters. Thus, in order to avoid even the slightest of interference of background noise, all measurements (present

as well as the ones reported in the earlier version of the manuscript) have been performed at a gain master of 833, as a consequence of which it may be considered that the images and blinking profiles shown in the manuscript are characteristics of luminescent particles and not of background. Please note that the images given as evidence of the integrity of our experimental approach are snapshots taken during the measurement.

In line with point 3 stated above, we have acquired the blinking profiles of Cys Au NCs and the corresponding background in the same frame and shown herein. It may be noted that the maximum intensity of the intermittency profile of the position containing Cys Au NCs was recorded to be ~ 1 unit. While negligible background noise was recorded for the corresponding background. The snapshots of the results are shown herein (Fig. S19).

(A)



Zooming the y axis of the intensity profile

(B)

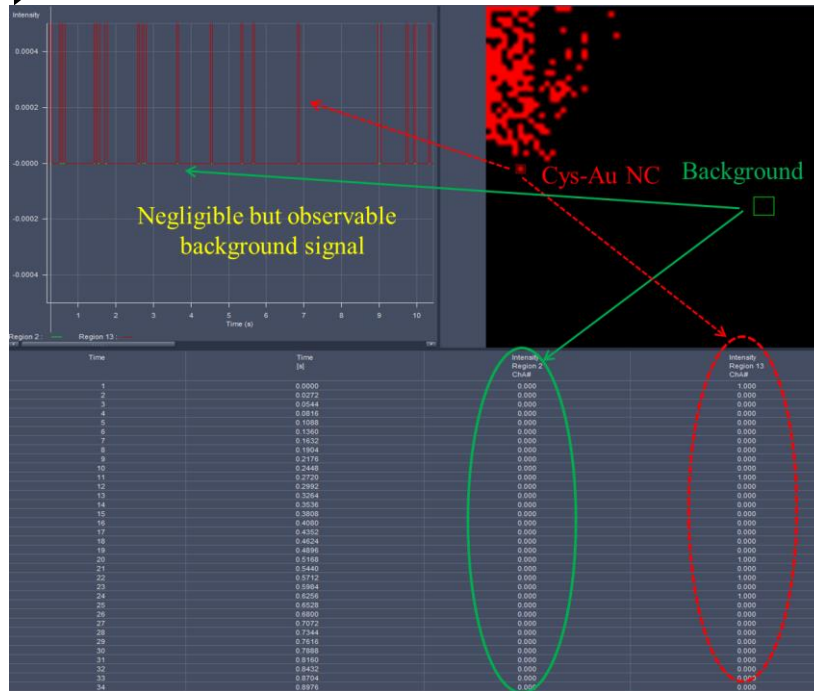


Fig. S19. (A) Screenshot of blinking profile of background plus Cys Au NCs and corresponding image of the area at which the blinking profile has been acquired, and corresponding table tabulating the intensity profile of blinking. **(B)** Zoomed version of **(A)**. Gain master was set at 833. Frame size was measured to be $64 \times 64 \mu\text{m}^2$

Thus, based on the above results, it may be considered unequivocally that the results given in the manuscript are due to intermittency characteristics of Cys Au NCs and are not due to detector noise.

Experimental results and explanations to substantiate the possible single particle nature of Cys Au NCs (assembled into a particle)

(1) Calculation of diffraction limited size of the laser focus:

Diffraction limited size of the laser focus = $(1.22 \times \lambda) / \text{NA}$; where NA = numerical aperture = 1.4 for confocal microscope (make: Zeiss LSM 880) and λ = wavelength of the laser = 355 nm. Thus, diffraction limited size of the laser focus = 0.309 μm .

(2) Single particle level quantum yield was calculated to corroborate the possible single particle nature of Cys Au NCs and Zn Cys Au NCs (assembled into a particle). The details of the calculation are as follows:

Calculation of quantum yield of Cys Au NCs and Zn Cys Au NCs at a single particle level:

The absorption cross sections of Cys Au NCs, Zn Cys Au NCs and rhodamine 6G (Rh6G) were calculated. In order to do so, the absorption coefficients of Cys Au NCs, Zn Cys Au NCs and Rh6G were calculated from a plot of absorbance versus concentration of the samples. The absorbance of the samples varied linearly with their concentrations (as per Lambert Beer's law).

The value of the absorption coefficient was extracted from the slope of the plot, keeping the path length fixed for all the measurements. The absorption coefficients for Cys Au NCs, Zn Cys Au NCs and Rh6G were calculated to be 5.63×10^{-3} , 5.58×10^{-3} , and $5.28 \times 10^{-5} \mu\text{M}^{-1}\text{cm}^{-1}$ respectively (Fig.s S20 A-C).

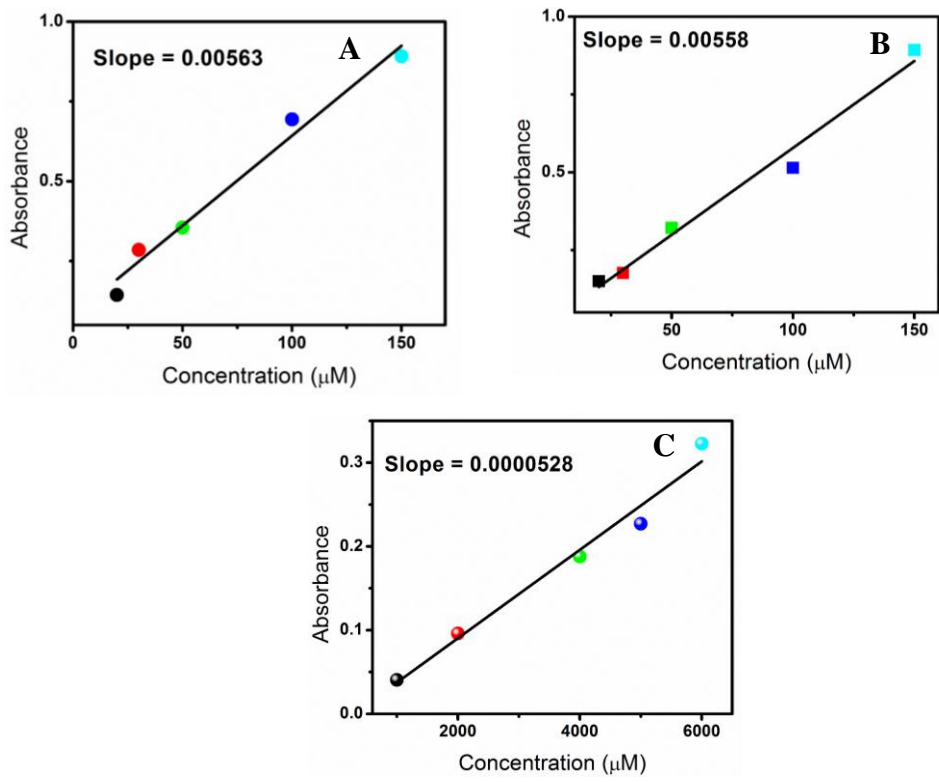


Fig. S20: Plot of Absorbance versus Concentration for (A) Cys-Au NCs, (B) Zn-Cys-Au NCs and (C) Rh6G.

Calculation of quantum yield for Cys Au NCs at single particle level:

$$\epsilon_{\text{Cys Au NCs}} = 0.00563 \mu\text{M}^{-1}\text{cm}^{-1}$$

Thus absorption cross section of Cys Au NCs = $(0.00563)/(6.023 \times 10^{23}) = 9.34 \times 10^{-27} \text{ cm}^2$

Similarly, $\epsilon_{\text{Rh6G}} = 0.0000528 \mu\text{M}^{-1}\text{cm}^{-1}$

Thus absorption cross section of Rh6G = $(0.0000528)/(6.023 \times 10^{23}) = 8.76 \times 10^{-29} \text{ cm}^2$

Mean intensity of 10 particles consisting of Cys Au NCs was calculated (using image J) to be 13.23.

On the other hand, mean intensity of 10 particles consisting of Rh6G was calculated (using image J) to be 13.74. Thus quantum yield of Cys Au NCs is given by:

$$QY = QY_{\text{reference}} \times (\text{Intensity}_{\text{sample}}/\text{Intensity}_{\text{reference}}) \times (\text{Absorption cross section}_{\text{reference}}/\text{Absorption cross section}_{\text{sample}}) \times (\text{refractive index of sample}/\text{refractive index of reference})$$

Given $QY_{\text{reference}} = 0.95$, and refractive indices for reference and sample are same,

QY of Cys Au NCs = $0.008 = \mathbf{0.8\%}$. This value is the upper limit of the quantum yield.

On the other hand, the quantum yield of Cys Au NCs in solution phase using Rh6G as a standard was calculated to be **0.2 %** by conventional methods. The deviation obtained in quantum yield calculation at a single particle level versus bulk phase could be attributed to the possible aggregation of more than one emitter Cys Au NCs) in one particle observed in CLSM analysis.

Calculation of quantum yield for Zn Cys Au NCs at single particle level:

$$\epsilon_{\text{Zn cys Au NCs}} = 0.00558 \mu\text{M}^{-1}\text{cm}^{-1}$$

Thus absorption cross section of Zn Cys Au NCs = $(0.00563)/(6.023 \times 10^{23}) = 9.34 \times 10^{-27} \text{ cm}^2$

Similarly, $\epsilon_{\text{Rh6G}} = 0.0000528 \mu\text{M}^{-1}\text{cm}^{-1}$

Thus absorption cross section of Rh6G = $(0.0000528)/(6.023 \times 10^{23}) = 8.76 \times 10^{-29} \text{ cm}^2$

Mean intensity of 10 particles consisting of Zn Cys Au NCs was calculated (using image J) to be 16.66.

On the other hand, mean intensity of 10 particles consisting of Rh6G was calculated (using image J) to be 13.74. Thus quantum yield of Zn Cys Au NCs is given by:

$$QY = QY_{\text{reference}} \times (\text{Intensity}_{\text{sample}}/\text{Intensity}_{\text{reference}}) \times (\text{Absorption cross section}_{\text{reference}}/\text{Absorption cross section}_{\text{sample}}) \times (\text{refractive index of sample}/\text{refractive index of reference})$$

Given $QY_{\text{reference}} = 0.95$, and refractive indices for reference and sample are same,

QY of Zn Cys Au NCs = **1.2%**. This value is the upper limit of the quantum yield.

On the other hand, the quantum yield of Zn Cys Au NCs in bulk phase using Rh6G as a standard was calculated to be **0.5 %** by conventional methods. The deviation obtained in quantum yield calculation at a single particle level versus bulk phase could be attributed to the possible aggregation of more than one emitter Zn Cys Au NCs) in one particle observed in CLSM analysis.

Table S4. Tabulation of the values of quantum yield at single particle level and bulk phase

Samples	Reference	Quantum Yield (%)	
		Bulk phase	Single particle
Cys-Au NCs	Rhodamine 6 G	0.2	0.8
Zn-Cys-Au NCs		0.5	1.2

(3) The density of the luminescent spots in a particular frame was found to be proportional with concentration of samples used for the measurements.

(4) As it may be noted in Fig. 1 (B1), (B2) and (B3), the photo bleaching occurred in a single step rather than via a monotonically decreasing intensity. In order to affirm this, a control experiment was performed where the blinking profile of a portion containing aggregated clusters was acquired. The observed profile demonstrated gradual photo bleaching owing to the presence of multiple particles. Please refer to Fig. S6, SI.

Profiles of Detector Noise acquired at various gain masters.

The blinking profiles of only background were also acquired. As already mentioned, the background noise could be adjusted by tuning the value of gain master, the background profiles have been acquired at two different gain master values – i.e., (i) 833, at which no background noise could be detected and hence all measurements in the reported manuscript had been done at that value and at (ii) 1000, the only value at which insignificant but low detector noise could be detected. The results are shown below (Fig. S21-S22):

intensity profile of blinking. **(B)** Zoomed version of **(A)**. Gain master was set at 833. Frame size was measured to be $64 \times 64 \mu\text{m}^2$

Gain master set at 1000:

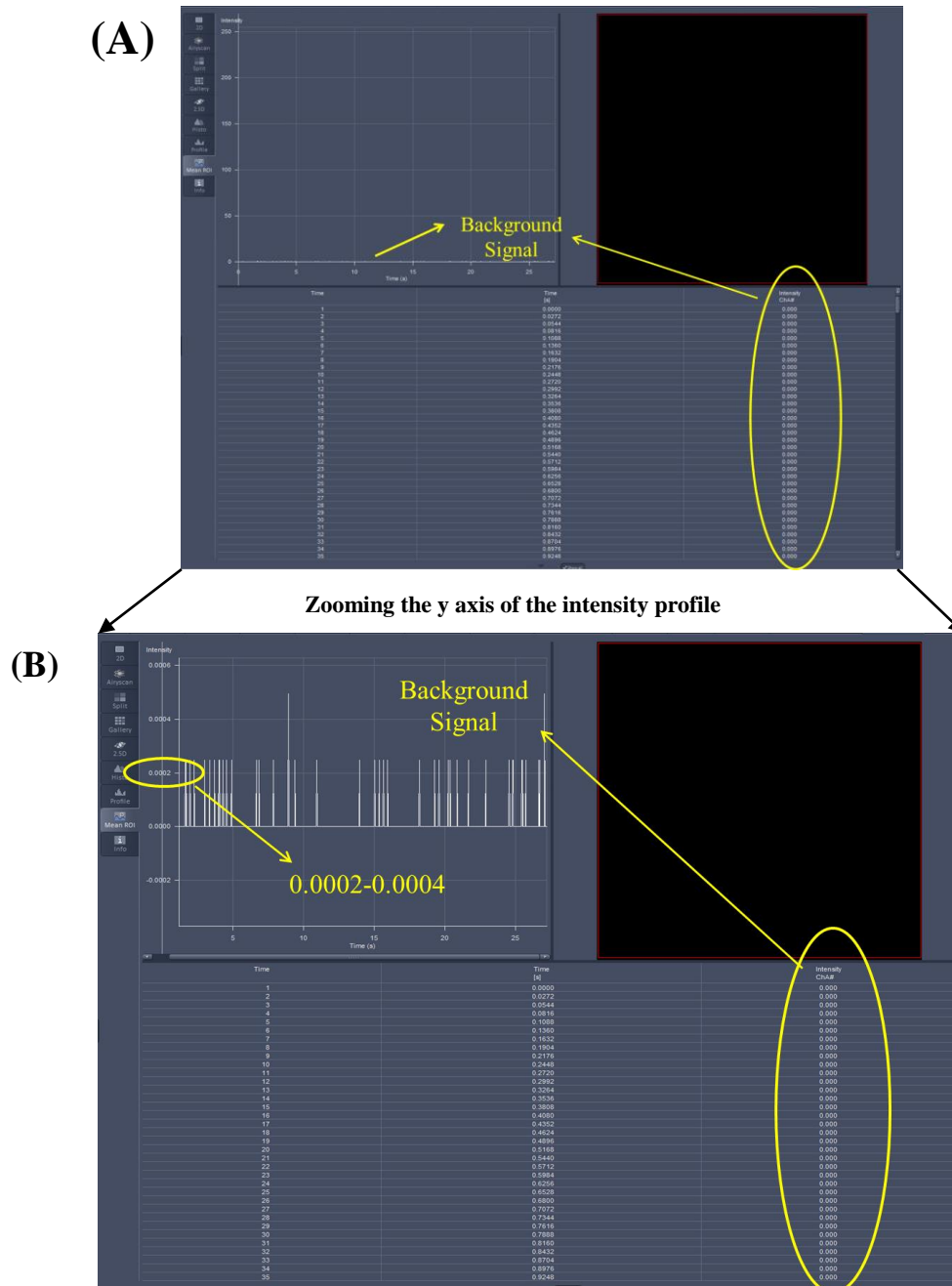


Fig. S22: **(A)** Screenshot of blinking profile of background and the corresponding image of the area at which the blinking profile has been acquired, and the corresponding table tabulating the

intensity profile of blinking. **(B)** Zoomed version of **(A)**. Gain master was set at 1000. Frame size was measured to be $64 \times 64 \mu\text{m}^2$

However, it is important to note here that at 1000 gain master, despite visual observation of some weak signals (intensity $\sim 10^{-4}$), the numerical values of the intensity were tabulated to be zero as the instrument is equipped to report intensity values till third decimal place.

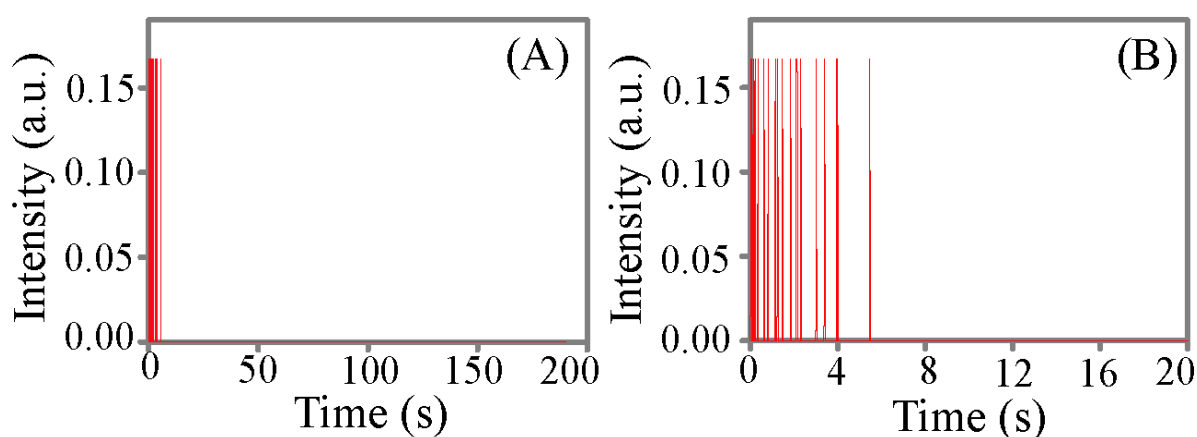


Fig. S23: **(A)** Blinking profile of Cys Au NCs acquired for 189 seconds. **(B)** The same profile as shown in **(A)** plotted at a time scale of 20 seconds.

Explanation for the observation of truncated power law in terms of off time distribution.

As it may be noted in reference 5, instead of a single state, exist for excited states and dark states in case of Au nanoclusters. Thus, transition of a photo excited electron to dark states will have different rate instead of a single unique rate, thereby accounting for the distributed kinetics observed for “off time distribution” of Au NCs.

Here it may be considered that the emissive surface states, like dark states, are also multiple in nature rather than a single one and hence would also invoke distributed kinetics. However, our observed unique on time value of 27 ms is indicative of a fixed on cycle probably

from a single state. This has been explained on the basis of the fact that the emissive surface states are essentially metal ligand emission state. In the present case, for all three different clusters (stabilized by cysteine, tryptophan and histidine) a common on time of 27 ms has been observed. Also, the common ligand stabilizing all three clusters is mercaptopropionic acid (MPA). Thus the metal ligand emission state in all three clusters is likely to arise from MPA-gold interactions. Also, it may be considered that apart from MPA, an additional ligand (amino acid) is also attached to the clusters. Thus, a question may arise as to why the latter would not constitute an emissive state. A probable answer to this question may emerge from the concept of soft-hard acid base theory. MPA is a thiolated ligand and owing to the high polarizability of sulphur (hence being soft in nature) charge transfer to soft Au is highly favourable. On the other hand, in case of tryptophan and histidine, the Au atoms of the clusters upon interaction with nitrogen has less scope for charge transfer owing to hard nature of nitrogen and soft nature of Au. Instead, the coordination of Au-N is likely to give rise to a dark state in the clusters owing to low oscillator strength. The case of Cys Au NCs is a little different from histidine and tryptophan stabilized Au NCs as the former (cysteine) is also a thiolated ligand. Despite being a thiolated ligand, it is important to note that cysteine, unlike MPA, has an amine group which being in close vicinity with Au atoms and upon interaction with Au atoms of the clusters may give rise to a dark state. Also, the number of cysteine per Au clusters (4) is much less than the number of MPA per clusters (10). Hence the existence of an emissive state due to cysteine-Au interaction is less compared to MPA-Au interaction. Thus, a single unique on state is expected for all three clusters owing to Au NCs-MPA interaction. Also, due to the presence of three different amino acids on Au NCs, the dark states are likely to be of different energies, as a consequence of which

the power law exponent for off time distribution in all the three different clusters have been obtained to be different (Table S2).

The “off time” distribution in case of Cys Au NCs, Trp Au NCs and His Au NCs could be fitted with a truncated power law. Thus, in all three cases, the power law behavior had an exponential falloff. This could be due to the presence of dark state(s) corresponding to longer “off time” in all three types of clusters, where the rate of transition of photo excited electrons is constant and is not governed by a distributed kinetics.

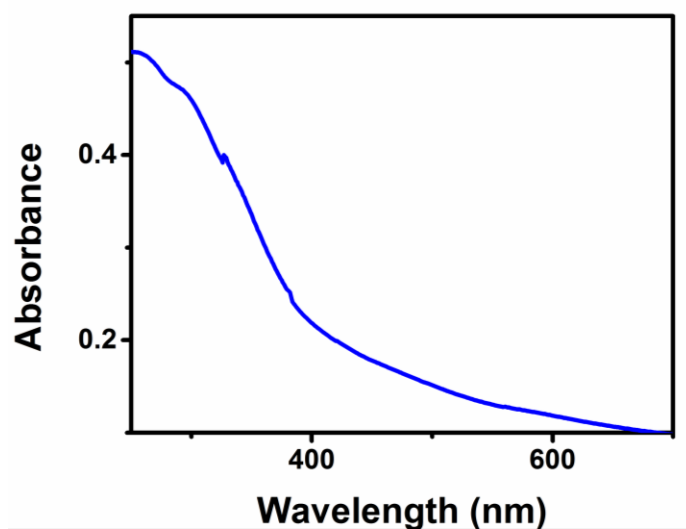


Fig. S24: UV-Vis absorption spectrum of Zn Cys Au NCs.

Control experiments and explanations to eliminate the interference of detector noise in the intermittency signals of Zn Cys Au NCs

In the CLSM model used for pursuing the current study (Zeiss LSM 880), range indicator is used to specify the area of luminescence and that of background in a particular frame of measurement. By default, red portions indicate non-zero or high pixel values and blue portions are indicative of zero pixel values.³

Also, in the confocal setup (LSM 880), gain master is adjusted to maximize the signal to noise ratio in a particular measurement. Herein, an optimised gain master of value 833 has been used to eliminate the background noise and acquire noise free images.

Thus we have recorded the CLSM image of Zn Cys Au NCs along with background with the range indicator being enabled. Interestingly, the area comprising of the clusters appeared red and the background (where absence of crystalline assembly of clusters was anticipated visually) appeared blue (Fig. S25 A-B). It is to be noted here that the red portion is indicative of a luminescent signal and is not a characteristic emission colour of the clusters.

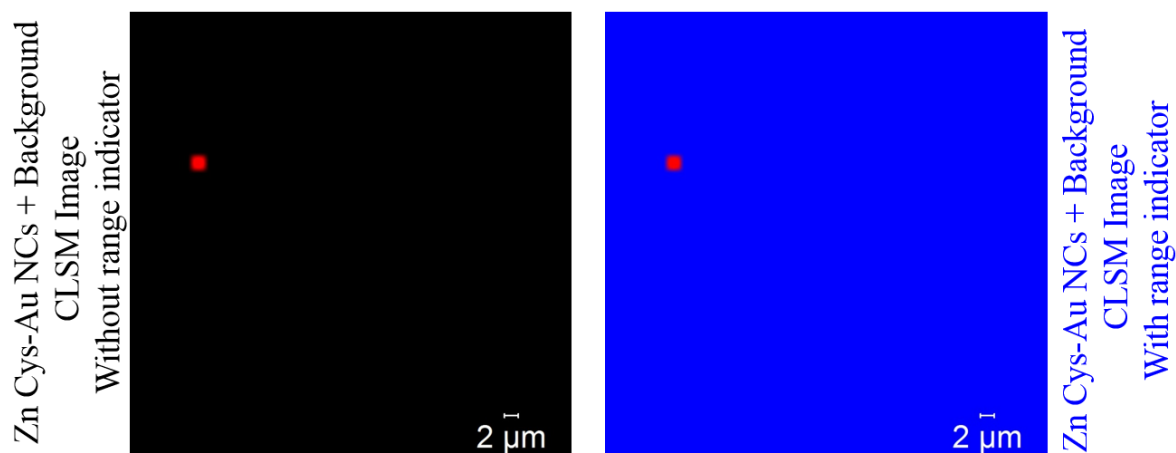


Fig. S25. (A) Confocal laser scanning microscopic image of Zn Cys Au NCs in presence of background (B) Corresponding image Zn Cys Au NCs in presence of background with range indicator being enabled.

Secondly, in order to establish that the reported images and the blinking profiles are typical signatures of the luminescent crystalline assemblies of clusters, we have acquired the

luminescent spectrum on a typical particle of Zn Cys Au NCs. Similarly, we have acquired the spectrum of the background in the same frame as that of the clusters. It is worthy to be mentioned here that the acquisitions have been done at a gain master value of 833. This value was optimized to completely eliminate the interference of background. Details of the optimization process has been discussed in the earlier section. Interestingly, in case of Zn Au NCs, the spectrum matched exactly with that of the solution phase, exhibiting an emission maximum at 590 nm. On the other hand, the spectrum acquired on the background was devoid of any characteristic peak at ~ 590 nm (Fig. S26).

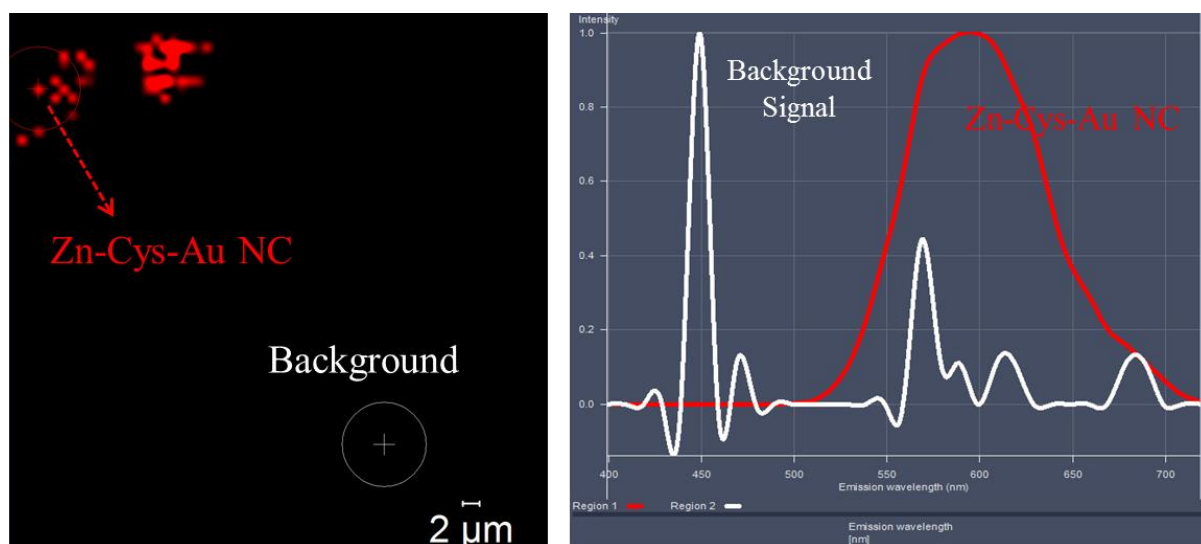


Fig. S26. (A) CLSM image of Zn Cys Au NCs (B) Corresponding spectra acquired on the regions marked in (A). The instrument displays the emission spectrum in the scale of 1.0 for all measurements.

We have acquired the blinking profiles of Zn Cys Au NCs and the corresponding background in the same frame and have shown herein. It may be noted that the intermittency

profile of the position containing Zn Cys Au NCs could be identified unambiguously in presence of the negligible background noise recorded for the corresponding background. The snapshots of the results are shown herein (Fig. S27).

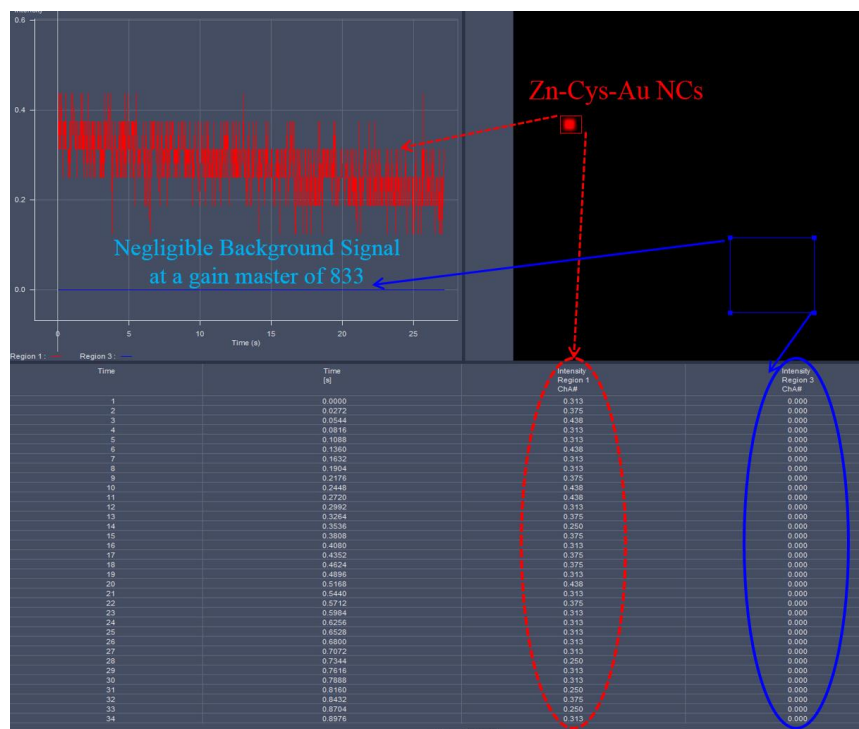


Fig. 27. (A) Screenshot of blinking profile of background plus Zn Cys Au NCs and the corresponding image of the area at which the blinking profile has been acquired, and the corresponding table tabulating the intensity profile of blinking. (B) Zoomed version of (A). Gain master was set at 833. Frame size was measured to be $64 \times 64 \mu\text{m}^2$

Explanation for proposing zinc as the plausible site Storage of CO₂ in Zn Cys Au NCs

It has been proposed in the manuscript that zinc ions are the potential sites for storage of CO₂. In order to substantiate this, we had provided the results of control experiments - the effect of CO₂ on ligand stabilized Cys-Au NCs (without zinc ions). Interestingly, no significant effect of CO₂ was observed on the luminescence of Cys-Au NCs (Fig. S13-S14). This indicated

the critical role of zinc ions in storage of CO₂. But it may be argued here that the properties of non assembled clusters may be different from that of assembled ones and hence non assembled clusters, in absence of an assembling agent, could not store CO₂. However, to address this issue and to further highlight the crucial role of zinc ions in storage and sensing of CO₂, we had synthesised ionic assembly of gold clusters mediated by sodium ions. Intriguingly, a typical particle of consisting sodium assisted assembly of Cys Au NCs (Na-Cys Au NCs), analogous to Zn Cys Au NCs, exhibited non blinking behaviour, which affirmed the formation of assembly of the clusters (Fig. S28 A). However, upon purging with CO₂, no change in blinking behavior of Na-Cys Au NCs was observed (Fig. 28 B). This confirmed that zinc ions played an important role in storage and sensing of CO₂.

It is evident from Fig. 2 E, that the ratio of Au:Zn is 1:2. Thus the chemical formula of the assembly could be written as Au₁₄MPA₁₀Cys₄Zn₂.

As per the proposed structure, the molecular weight of the crystalline assembly is:

$$14 \times \text{Au} + 10 \times \text{MPA} + 4 \times \text{Cys} + 2 \times \text{Zn} = 4408$$

As zinc is proposed to be the active centre for storage of CO₂, (2 × Zn) = 130 g in 4408 gram is effective for storage of CO₂.

Therefore, in 1 g, 0.029 g is effective for storage of CO₂.

0.029 g of zinc corresponds to 0.00045 M = 0.45 mM.

Now, since in per unit cell (containing 2 zinc ions) (Fig. 2 E), one zinc ion is tri coordinated (with MPA), thus can further coordinate to three CO₂, and the other being bi coordinated (with Cys) can further coordinate to 4 CO₂ (in order to achieve maximum coordination of 6), total 7 CO₂ can be incorporated in a unit lattice of Zn Cys Au NCs.

Thus unit equivalence of zinc to CO₂ is 2:7

Therefore, for 0.4 mM of zinc ions present in the lattice, $(0.45 \times 7)/2 = 1.575$ mM of CO₂ can be stored per gram of Zn Cys Au NCs. This closely matches with our observed value of 1.79 mM of CO₂ stored per gram of Zn Cys Au NCs.

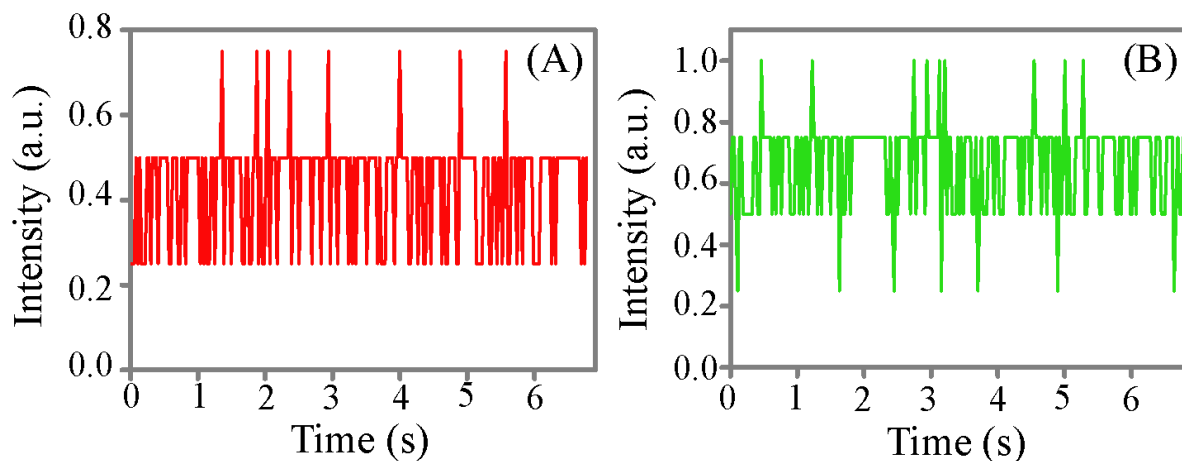


Fig. S28: (A) Blinking profile of Na-Cys Au NCs at 0% CO₂. (B) Blinking profile of Na-Cys Au NCs at 4.7% CO₂.

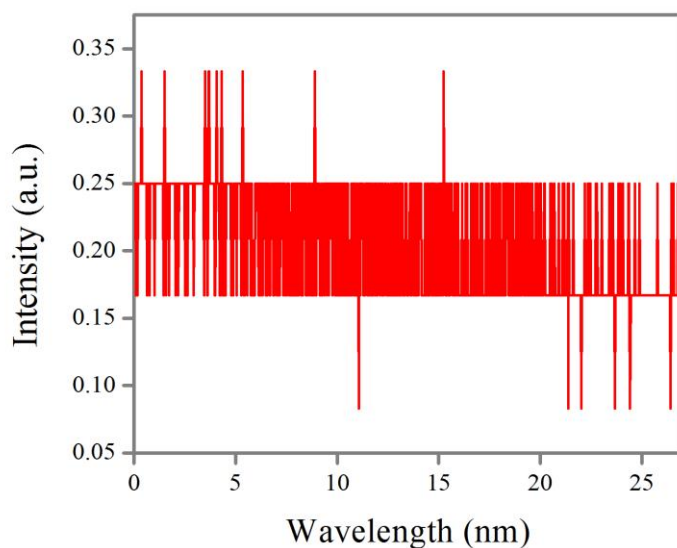


Fig. S29: Additional representative blinking profile of Cys Zn Au NCs corresponding to Video S11.

References:

1. M. A. Tofanelli, C. J. Ackerson, *J. Am. Chem. Soc.*, 2012, 134, 16937-16940
2. Lechtken, A; Neiss, C.; Kappes, M. M.; Schooss, D. Structure determination of gold clusters by trapped ion electron diffraction: Au₁₄⁻-Au₁₉⁻. *Phys. Chem. Chem. Phys.* **2009**, *11*, 4344-4350.
3. web.path.ox.ac.uk/~bioimaging/Documents/Zeiss_880_User_guide.pdf
4. Yau, S. H.; Varnavski, O.; Gilbertson, J. D.; Chandler, B.; Ramakrishna, G.; Goodson, T., Ultrafast Optical Study of Small Gold Monolayer Protected Clusters: A Closer Look at Emission. *J. Phys. Chem. C* **2010**, *114*, 15979-15985.
5. Yau, S. H.; Ashenfelter, B. A.; Desireddy, A.; Ashwell, A. P.; Varnavski, O.; Schatz, G. C.; Bigioni, T. P.; Goodson, T., Optical Properties and Structural Relationships of the Silver Nanoclusters Ag₃₂(SG)₁₉ and Ag₁₅(SG)₁₁. *J. Phys. Chem. C* **2017**, *121*, 1349-1361.